

The precession of orbital plane and the secular variabilities of binary pulsars

B.P. Gong

*Department of Astronomy, Nanjing University, Nanjing 210093, P.R.China**

In Barker and O’Connell’s gravitational two body equation, the total angular momentum of a binary system is defined as the sum of the orbital angular momentum and the angular momenta of two spins. This paper point out that actually Barker and O’Connell’s orbital precession velocity is contradictory to this definition. This paper makes the definition as a geometry constraint, and imposes it on the equation of motion of Barker and O’Connell’s two body equation. And obtains the spin orbit coupling induced orbital precession velocity as well as the advance of precession of periastron of a binary pulsar system through perturbation method. The predicted effects is consistent with a theory independent result. Moreover by applying the predicted effects to four typical binary pulsars, PSR J2051-0827, PSR B1957+20, PSR J1012+5307, and PSR J1713+0747, the significant secular variabilities can be well interpreted.

PACS numbers: 04.80.-y, 04.80.Cc, 97.10.-q

I. INTRODUCTION

Barker and O’Connell (BO) [1] first gave the gravitational two-body equation with spins. In which the precession velocity of the two spins, the equation of motion and the orbital angular momentum are given. Damour and Schäfer [2] derive Barker and O’Connell’s orbital precession velocity in a simple manner.

In the application to pulsar timing measurement, Smarr and Blandford[3], Lai et al[4], Wex and Kopeikin[5] decompose the orbital precession velocity of BO’s along two vectors, the total angular momentum vector, \mathbf{J} , and the orbital angular momentum vector, \mathbf{L} . Thus the spin orbit (S-L) coupling induced precession velocity of the orbital plane, $\dot{\Phi}_S$, and the advance of precession of periastron, $\dot{\Psi}_S$, are obtained. In which the magnitude of $\dot{\Psi}_S$ is 1 Post-Newtonian order (PN). Whereas, Apostolatos et al[6] obtained the corresponding result through a method independent of the the orbital precession velocity, which gives $\dot{\Psi}_S$ of 1.5PN.

And in confrontation with observation, the predicted secular variabilities, concerning the advance of precession of periastron, like \dot{P}_b , is much smaller than that of the corresponding observations. Some authors uses other effects to interpret such significant variabilities. However the explanation is not very successful for binary pulsars with large orbital period, i.e., for days; and higher order of derivatives measured on some binary pulsars cannot be well explained.

This paper point out that the reason of the two inconsistencies is that BO equation actually contradictory to BO’s definition: $\mathbf{J} = \mathbf{L} + \mathbf{S}$ (where \mathbf{S} is the sum of spin angular momenta of two stars), which prevents BO equation from obtaining a correct orbital precession velocity, and therefore, correct secular effects to explain observations of binary pulsars.

On the other hand, in the study of S-L coupling effect on the modulation of the gravitational wave from merging binaries, Apostolatos et al[6] and Kidder (AK)[7] obtain an orbital precession velocity that satisfies $\mathbf{J} = \mathbf{L} + \mathbf{S}$. This paper shows that if AK’s velocity is also decomposed, then the obtained $\dot{\Phi}_S$ and $\dot{\Psi}_S$ can be consistent with the velocity independent result given by Apostolatos et al.

To obtain a unique solution to the precession of \mathbf{L} , BO assumes that \mathbf{L} precesses at the same velocity as the Runge-Lenz vector, \mathbf{A} . It is this assumption that make the precession velocity of \mathbf{L} contradictory to the definition, $\mathbf{J} = \mathbf{L} + \mathbf{S}$. Whereas, AK’s orbital precession velocity is obtained without such assumption, therefore, it is consistent with the definition.

BO and AK are based on the same Hamiltonian of S-L coupling and the same precession velocity of the angular momenta of the two spins. However BO’s orbital precession velocity is not a self-consistent one, while AK’s is self-consistent. And in the application to pulsar timing observation, the two kinds of orbital precession velocities correspond to very different results, i.e., 4 order of magnitude discrepancy for some secular parameters.

This paper uses the definition of $\mathbf{J} = \mathbf{L} + \mathbf{S}$ as a geometry constraints, imposing it on BO’s equation of motion, and use perturbation to obtain the S-L coupling induced orbital precession velocity and advance of precession of periastron of a binary pulsar system. The result can be consistent that of Apostolatos et al’s[6]. Moreover in the application to pulsar timing measurement, the predicted effect can explain not only the first derivative of the projected semi-major axes, \dot{x} , but also \ddot{x} , \dot{P}_b , and \ddot{P}_b of four typical binary pulsars, PSR J2051-0827, PSR B1957+20, PSR J1012+5307, and PSR J1713+0747.

The arrangement is as follows: Sec II introduces the derivation of orbital precession velocity of BO and AK. The corresponding scenarios of the two kinds of orbital precession velocity are compared. And why BO’s orbital precession velocity violates the definition of \mathbf{J} is analyzed. Sec III compares the differences between BO and AK’s orbital precession velocity when they are de-

*Electronic address: bpgong@nju.edu.cn

composed into two components, along \mathbf{L} and along \mathbf{J} respectively. It is shown that one of the two components of BO's cannot be consistent with the independent result of given by Apostolatos et al[6].

In Sect IV, $\mathbf{J} = \mathbf{L} + \mathbf{S}$ is used as a geometry constraints, by imposing it on BO's equation of motion, the S-L coupling induced orbital precession velocity and advance of precession of periastron are obtained through perturbation method in celestial mechanics. The result can be consistent that of Apostolatos et al's[6]. Sect V drives secular variabilities caused by S-L coupling induced effect. The secular effects derived from equations that satisfies the constraint and violate the constraint are compared with observation in Sect VI. Sect VII concludes that whether $\mathbf{J} = \mathbf{L} + \mathbf{S}$ is satisfied or not, can cause very different predictions on the secular parameters of a binary pulsar system, although all derivations start from the same point, general relativity.

II. ORBITAL PRECESSION VELOCITY

This section introduces the derivation of the orbital precession velocity of BO and AK, analyzes two different scenarios corresponding to BO and AK's orbital precession velocity, and points out that BO's orbital precession velocity actually violates the definition of the total angular momentum of a binary system.

A. derivation of BO's orbital precession velocity

The total Hamiltonian for the gravitational two-body problem with spin is given by [1, 2],

$$H = H_N + H_{1PN} + H_{2PN} + H_S, \quad (1)$$

where H_N , H_{1PN} and H_{2PN} are the Newtonian, the first and second order post-Newtonian terms respectively. H_S is the spin-orbit interaction Hamiltonian [1, 2],

$$H_S = \sum_{\alpha=1}^2 (2 + 3 \frac{m_{\alpha+1}}{m_\alpha}) (\frac{\mathbf{S}_\alpha \cdot \mathbf{L}}{r^3}), \quad (2)$$

where $\alpha + 1$ is meant modulo 2 ($2+1=1$), m_1 , m_2 are the masses of the two stars, respectively, $r = a(1 - e^2)^{1/2}$, a is the semi-major axes, e is the eccentricity of the orbit. Notice this paper uses $G = c = 1$. \mathbf{S}_1 and \mathbf{S}_2 are the spin angular momenta of star 1 and star 2 respectively. The secular result for \mathbf{S}_1 is given [1],

$$\begin{aligned} \dot{\hat{\Omega}}_1 = & \frac{L(4 + 3m_2/m_1)}{2r^3} \hat{\mathbf{L}} + \frac{S_2}{2r^3} [\hat{\mathbf{S}}_2 - 3(\hat{\mathbf{L}} \cdot \hat{\mathbf{S}}_2) \hat{\mathbf{L}}] \\ & + \frac{m_2 m_1 J_2^{(1)}}{2S_1 r^3} [\hat{\mathbf{S}}_1 - 3(\hat{\mathbf{L}} \cdot \hat{\mathbf{S}}_1) \hat{\mathbf{L}}], \end{aligned} \quad (3)$$

where $\hat{\mathbf{L}}$, $\hat{\mathbf{S}}_1$ and $\hat{\mathbf{S}}_2$ are unit vectors of the orbital angular momentum, the spin angular momentum of star 1 and star 2, respectively. The quadrupole from the rotational distortion of the finite sized companion is specified by the difference between the moments of inertia about the spin axis, I_3 and an orthogonal axis, I_1 [1, 4].

$$m_1 J_2^{(1)} = I_3 - I_1, \quad (4)$$

$\dot{\hat{\Omega}}_2$ can be obtained by exchanging the subscript 1 and 2 at the right side of Eq(3). The first term of Eq(3) represents the geodetic (de Sitter) precession, which corresponds to the precession of \mathbf{S}_1 around \mathbf{L} , it is 1PN due to $\frac{L}{r^3} \sim (\frac{v}{c})^2 (\frac{v}{r})$; and the second term represents the Lense-Thirring precession, \mathbf{S}_1 around \mathbf{S}_2 , which is $\frac{S}{L}$ times smaller than the first, therefore, it corresponds to 1.5PN. The third term at right hand side of Eq(3) corresponds to the precession of star 1 induced by the coupling of the quadrupole moment of star 1 with the orbit.

BO equation describes the secular effect of the orbital plane by a rotational velocity vector, $\hat{\Omega}_S$, acting on some instantaneous Newtonian ellipse. Damour and Schäfer [2] computed $\hat{\Omega}_S$ in a simple manner by making full use of Hamiltonian method.

The functions of the canonically conjugate phase space variables \mathbf{r} and \mathbf{p} are defined as

$$\mathbf{L}(\mathbf{r}, \mathbf{p}) = \mathbf{r} \times \mathbf{p}, \quad (5)$$

$$\mathbf{A}(\mathbf{r}, \mathbf{p}) = \mathbf{p} \times \mathbf{L} - GM\mu^2 \frac{\mathbf{r}}{r}, \quad (6)$$

where $M = m_1 + m_2$, $\mu = m_1 m_2 / M$. The vector \mathbf{A} is the Runge-Lenz vector (first discovered by Lagrange). The instantaneous Newtonian ellipse evolves according to the fundamental equations of Hamiltonian dynamics [2]

$$\dot{\mathbf{L}} = \{\mathbf{L}, H\}, \quad (7)$$

$$\dot{\mathbf{A}} = \{\mathbf{A}, H\}, \quad (8)$$

where $\{, \}$ denote the Poisson bracket. \mathbf{L} and \mathbf{A} are first integrals of H_N , only $H_{1PN} + H_{2PN} + H_S$ contributes to the right-hand sides of Eq(7) and Eq(8), in which $H_{1PN} + H_{2PN}$ determines the precession of periastron,

$$\dot{\omega}^{GR} = \frac{6\pi M}{P_b a (1 - e^2)}, \quad (9)$$

where P_b is the orbital period. To study the spin-orbit interaction, it is sufficient to consider H_S . Thus replacing H of Eq(7) and Eq(8) by H_S obtains [2],

$$\left(\frac{d\mathbf{L}}{dt}\right)_S = \{\mathbf{L}, H_S\} = \dot{\hat{\Omega}}_S^* \hat{\mathbf{S}} \times \mathbf{L}, \quad (10)$$

$$\left(\frac{d\mathbf{A}}{dt}\right)_S = \{\mathbf{A}, H_S\} = \dot{\hat{\Omega}}_S^* [\hat{\mathbf{S}} - 3(\hat{\mathbf{L}} \cdot \hat{\mathbf{S}}) \hat{\mathbf{L}}] \times \mathbf{A}. \quad (11)$$

In Damour and Schäfer's equation [2], \mathbf{S} represents a linear combination of \mathbf{S}_1 and \mathbf{S}_2 . For simplicity of discussion, and for consistence with Wex and Kopeikin [5]'s application of $\dot{\Omega}_S$, we assume $\mathbf{S} = \mathbf{S}_1$ (the other spin angular momentum is ignored) until Sec IV where general binary pulsar is discussed.

$$\dot{\Omega}_S^* = \frac{S(4 + 3m_2/m_1)}{2r^3} . \quad (12)$$

The solution of Eq(10) and Eq(11) gives the S-L coupling induced orbital precession velocity [2]

$$\dot{\Omega}_S = \dot{\Omega}_S^* [\hat{\mathbf{S}} - 3(\hat{\mathbf{L}} \cdot \hat{\mathbf{S}})\hat{\mathbf{L}}] . \quad (13)$$

From Eq(13), the first derivative of $\hat{\mathbf{L}}$ can be obtained,

$$\frac{d\hat{\mathbf{L}}}{dt} = \dot{\Omega}_S^* \hat{\mathbf{S}} \times \hat{\mathbf{L}} , \quad (14)$$

and from Eq(3) the first derivative of $\hat{\mathbf{S}}$ (recall $\mathbf{S} = \mathbf{S}_1$) can be written

$$\frac{d\hat{\mathbf{S}}}{dt} = \dot{\Omega}_1^* \hat{\mathbf{L}} \times \hat{\mathbf{S}} = \Omega_S^* \frac{L}{S} \hat{\mathbf{L}} \times \hat{\mathbf{S}} , \quad (15)$$

where $\dot{\Omega}_1^*$ is the first term at the right hand side of Eq(3). Eq(14) and Eq(15) actually corresponds to such a scenario of motion of a binary pulsar system, that $\hat{\mathbf{L}}$ precesses slowly around $\hat{\mathbf{S}}$, 1.5PN, as shown by Eq(14); whereas $\hat{\mathbf{S}}$ precesses rapidly around $\hat{\mathbf{L}}$, 1PN, as shown in Eq(15). Therefore BO equation predicts that the two vectors, $\hat{\mathbf{L}}$ and $\hat{\mathbf{S}}$ precess around each with very different precession velocities (typically one is larger than the other for 3 to 4 order of magnitude for a general binary pulsar system).

B. orbital precession velocity in the calculation of gravitational wave

In the study of the modulation of precession of orbital plane to gravitational wave, the orbital precession velocity is obtained in a different manner and the result is very different from that given by Eq(13).

Since the gravitation wave corresponding to 2.5PN, which is negligible comparing to S-L coupling effect that corresponds to 1PN and 1.5PN, the total angular momentum can be treated as conserved, $\dot{\mathbf{J}} = 0$. Then following equation can be obtained[1],

$$\dot{\Omega}_0 \times \mathbf{L} = -\dot{\Omega}_1 \times \mathbf{S}_1 - \dot{\Omega}_2 \times \mathbf{S}_2 . \quad (16)$$

Notice that as defined by BO[1] and AK[6, 7], $\mathbf{L} = \mu M^{1/2} r^{1/2} \hat{\mathbf{L}}$. In the one spin case the right hand side of Eq(16) can be given [7],

$$\dot{\mathbf{S}} = \frac{1}{2r^3} (4 + \frac{3m_2}{m_1}) (\mathbf{L} \times \mathbf{S}) . \quad (17)$$

Considering $\mathbf{J} = \mathbf{L} + \mathbf{S}$, Eq(17) can be written,

$$\dot{\mathbf{S}} = \frac{1}{2r^3} (4 + \frac{3m_2}{m_1}) (\mathbf{J} \times \mathbf{S}) . \quad (18)$$

Similarly, the left hand side of Eq(16) can be given,

$$\dot{\mathbf{L}} = \frac{1}{2r^3} (4 + \frac{3m_2}{m_1}) (\mathbf{J} \times \mathbf{L}) . \quad (19)$$

By Eq(18) and Eq(19), \mathbf{L} and \mathbf{S} precess about the fixed vector \mathbf{J} at the same rate with a precession frequency approximately [7]

$$\dot{\Omega}_0 = \frac{|\mathbf{J}|}{2r^3} (4 + \frac{3m_2}{m_1}) . \quad (20)$$

Eq(20) indicates that in 1 PN approximation, $\hat{\mathbf{L}}$ and $\hat{\mathbf{S}}$ can precess around \mathbf{J} rapidly (1PN) with exactly the same velocity. Notice that the misalignment angles between $\hat{\mathbf{L}}$ and $\hat{\mathbf{S}}$ (λ_{LS}), $\hat{\mathbf{L}}$ and $\hat{\mathbf{J}}$ (λ_{LJ}) are very different, due to $S/L \ll 1$, λ_{LJ} is much smaller than λ_{LS} .

Thus, Eq(19) and Eq(18) correspond to a very different scenario of motion of \mathbf{S} , \mathbf{L} and \mathbf{J} from that given by BO equation shown in Eq(14) and Eq(15).

C. comparison of two scenarios

The total angular momentum of a binary system is defined as [1]

$$\mathbf{J} = \mathbf{L} + \mathbf{S} , \quad (21)$$

Eq(21) means that \mathbf{J} , \mathbf{L} and \mathbf{S} form a triangle, and therefore, it guarantees that the three vectors must be in one plane at any moment.

For a general radio binary pulsar system, the total angular momentum of this system is conserved in 1PN order. Therefore we have

$$\dot{\mathbf{J}} = 0 . \quad (22)$$

Eq(22) means that \mathbf{J} is a constant during the motion of a binary system. Eq(22) and Eq(21) together provide a scenario that the triangle formed by \mathbf{L} , \mathbf{S} and \mathbf{J} determines a plane, and the plane rotates around a fixed axes, \mathbf{J} , with velocity $\dot{\Omega}_0$. This scenario is shown in Fig 1. which can also be represented as,

$$\dot{\mathbf{J}} = \dot{\Omega}_0 \hat{\mathbf{J}} \times \mathbf{L} + \dot{\Omega}_0 \hat{\mathbf{J}} \times \mathbf{S} = 0 , \quad (23)$$

Smarr and Blandford [3] mentioned the scenario as that \mathbf{L} and \mathbf{S} must be at opposite side of \mathbf{J} at any instant. Hamilton and Sarazin [8] also study the scenario and state that \mathbf{L} precesses rapidly around \mathbf{J} .

Obviously the orbital precession velocity given by Eq(20) can satisfy the two constraints, Eq(21) and Eq(22) simultaneously.

Can the BO's orbital precession velocity given by Eq(13) satisfy the two constraints, Eq(21) and Eq(22)

simultaneously? From Eq(13), Eq(14) and Eq(15), the first derivative of \mathbf{J} can be written [1]

$$\dot{\mathbf{J}} = \dot{\Omega}_S \times \mathbf{L} + \dot{\Omega}_1^* \times \mathbf{S} = \dot{\Omega}_S^* \hat{\mathbf{S}} \times \mathbf{L} + \dot{\Omega}_1^* \hat{\mathbf{L}} \times \mathbf{S} \equiv 0, \quad (24)$$

and since Eq(21) is defined in BO's equation [1], then it seems that BO equation can be satisfied both Eq(21) and Eq(22). However following analysis can show that BO's orbital precession velocity is actually contradictory to its definition of Eq(21).

If Eq(21) is truly satisfied, then we can use $\mathbf{L} = \mathbf{J} - \mathbf{S}$ and $\mathbf{S} = \mathbf{J} - \mathbf{L}$ to replace \mathbf{L} and \mathbf{S} at the right hand side of Eq(24) respectively, and therefore Eq(24) becomes,

$$\dot{\mathbf{J}} = \dot{\Omega}_S \times (\mathbf{J} - \mathbf{S}) + \dot{\Omega}_1^* \times (\mathbf{J} - \mathbf{L}) = 0, \quad (25)$$

$$\dot{\mathbf{J}} = -\dot{\Omega}_S^* \frac{\mathbf{J}}{S} \times \mathbf{S} - \dot{\Omega}_1^* \frac{\mathbf{J}}{L} \times \mathbf{L} = 0, \quad (26)$$

Then by the magnitude $\dot{\Omega}_S^*$ given by Eq(12), and $\dot{\Omega}_1^*$ given by Eq(3), one can find that Eq(26) is equivalent to Eq(23), which means that once the definition of Eq(21) is satisfied, Eq(24) can reduce to Eq(23).

However Eq(23) and Eq(20) correspond to the following orbital precession velocity,

$$\dot{\Omega}_0 = \dot{\Omega}_S^* (\hat{\mathbf{S}} + \frac{L}{S} \hat{\mathbf{L}}). \quad (27)$$

Obviously Eq(27) is not consistent with BO's Eq(13), which demands that the coefficient of the component along $\hat{\mathbf{L}}$ be $\gamma = -3(\hat{\mathbf{L}} \cdot \hat{\mathbf{S}})$. Whereas, Eq(27) corresponds to $\gamma = \frac{L}{S}$.

In other words, once Eq(21), the definition of BO, is satisfied, then BO's orbital precession velocity of Eq(13) must be violated. Therefore, BO's orbital precession velocity cannot be consistent with $\mathbf{J} = \mathbf{L} + \mathbf{S}$, which is defined by themselves [1].

Actually Eq(27) can be consistent with Eq(10), however it is contradictory to Eq(11). The reason of introducing Eq(11) is that without it, Eq(10) alone cannot determine a unique solution.

Eq(23) and Eq(20) can be regarded as solving this problem by using Eq(10) and Eq(21) instead of Eq(10) and Eq(11) to obtain the orbital precession velocity. In such case, the definition of Eq(21) is automatically satisfied.

As defined in Eq(5) and Eq(6), \mathbf{L} and \mathbf{A} are vectors which are determined by different elements in celestial mechanics, $\mathbf{L}(\Omega, i)$ and $\mathbf{A}(\Omega, i, \omega, e)$ respectively.

Therefore, \mathbf{L} and \mathbf{A} corresponds to different precession velocities, as given by Eq(10) and Eq(11) respectively. However since the discrepancy is only in $\hat{\mathbf{L}}$ component, which does not influence the satisfaction of the conservation equation, Eq(24), thus the discrepancy seems unimportant. And therefore, precession velocity of \mathbf{L} is treated equivalent to that of \mathbf{A} 's, thus the component in $\hat{\mathbf{L}}$ are both $\gamma = -3(\hat{\mathbf{L}} \cdot \hat{\mathbf{S}})$. Whereas, as given by Eq(27), the

corresponding component must be $\gamma = \frac{L}{S}$ if the triangle constraints be satisfied. Therefore, the violation of the triangle constraint is inevitable under the assumption that \mathbf{L} and \mathbf{A} precess at the same velocity.

The discrepancy in γ given by BO and AK is about 4 order of magnitude, which in turn, can cause around 4 order of magnitude discrepancy in some secular parameters for a general radio binary pulsar system. The current observation already provides many data to test the two different predictions.

III. COMPONENT OF ORBITAL PRECESSION VELOCITY

In the application to observation, Smarr and Blandford, Lai et al, Wex and Kopeikin decompose $\dot{\Omega}_S$ of Eq(13) given by BO into two components, the precession of the orbital plane, Φ , and the longitude of the periastron, Ψ , defined with respect to the invariable plane (the plane perpendicular to \mathbf{J}) and the orbital plane (the plane perpendicular to \mathbf{L}) respectively, as shown in Fig 2.

As analyzed in last section, since the orbital precession velocity, $\dot{\Omega}_S$ of Eq(13), is not a self-consistent velocity, the components derived from it would reflect this inconsistency.

The S-L coupling induced effect along \mathbf{J} and \mathbf{L} are represented by $\dot{\Psi}_S$ and $\dot{\Phi}_S$ respectively. $\dot{\Omega}_S$ of Eq(13) can be written as,

$$\dot{\Omega}_S = a \hat{\mathbf{L}} + b \hat{\mathbf{J}}, \quad (28)$$

through the triangle formed by \mathbf{L} , \mathbf{J} , \mathbf{S} , one can obtain a and b of Eq(28),

$$a = 2 \cos \lambda_{LS} - \sin \lambda_{LS} \cot \lambda_{LJ}, \quad b = \sin \lambda_{LS} \csc \lambda_{LJ}, \quad (29)$$

where λ_{LS} and λ_{LJ} are shown in Fig 2 and Fig 3. Then by Eq(13), Eq(28) and Eq(29), $\dot{\Phi}_S$ and $\dot{\Psi}_S$ are given [5],

$$\dot{\Phi}_S = \dot{\Omega}_S^* \left(\frac{\sin \lambda_{LS}}{\sin \lambda_{LJ}} \right), \quad (30)$$

$$\dot{\Psi}_S = \dot{\Omega}_S^* (2 \cos \lambda_{LS} - \sin \lambda_{LS} \cot \lambda_{LJ}), \quad (31)$$

Since that for a general binary pulsar, $\lambda_{LJ} \ll 1$ (due to $S/L \ll 1$), the second term at the right hand side of Eq(31) is much larger than that rest term (terms) at the right hand sides of Eq(31). Thus both $\dot{\Phi}_S$ and $\dot{\Psi}_S$ are 1PN.

Comparatively, if we decompose Eq(27) into two components, along $\hat{\mathbf{L}}$ and $\hat{\mathbf{J}}$ respectively, then the corresponding $\dot{\Phi}_S$ and $\dot{\Psi}_S$ are given,

$$\dot{\Phi}_S = \dot{\Omega}_0, \quad (32)$$

$$\dot{\Psi}_S = \dot{\Omega}_S^* \left(-\sin \lambda_{LS} \cot \lambda_{LJ} + \frac{L}{S} \right), \quad (33)$$

since $\frac{L}{S} = \frac{\sin \lambda_{LS}}{\sin \lambda_{LJ}}$, and by $\lambda_{LJ} \ll 1$, we have $\lambda_{LS} \approx \pi - \lambda_{JS}$. Thus Eq(33) can be written,

$$\dot{\Psi}_S = \dot{\Omega}_S^* (-\sin \lambda_{LS} \cot \lambda_{LJ} + \frac{\sin \lambda_{LS}}{\sin \lambda_{LJ}}) \sim O(c^{-5}). \quad (34)$$

Eq(34) means $\dot{\Psi}_S$ is 1.5PN. Therefore, there are two different approaches in obtaining $\dot{\Phi}_S$ and $\dot{\Psi}_S$, the first one is that Eq(10) and Eq(11) determine $\dot{\Omega}_S$, and in turn $\dot{\Omega}_S$ determines $\dot{\Phi}_S$ and $\dot{\Psi}_S$; the second one is: Eq(10) and Eq(21) determines $\dot{\Omega}_0$, and $\dot{\Omega}_0$ determines $\dot{\Phi}_S$ and $\dot{\Psi}_S$. The two methods predict same $\dot{\Phi}_S$, but very different $\dot{\Psi}_S$.

Apostolatos et al[6] (Eq(28)), calculated $\dot{\Psi}_S$, the Thomas precession term, through a method independent of BO equation, which gives $\dot{\Psi}_S \sim \dot{L}/L$ (Eq(28) of [6]), which is 1.5PN. Obviously Eq(34) is consistent with this result, whereas, Eq(31) is contradictory to it.

The discrepancy is due to the decomposing based on different orbital precession velocities, Eq(13) and Eq(20), respectively, which in turn is due to the different constraints used in obtaining the orbital precession velocity, as discussed in last section and as shown in Table I.

IV. $\dot{\Phi}_S$ AND $\dot{\Psi}_S$ BY PERTURBATION METHOD

In this section, the definition of \mathbf{J} is used a geometry constraint to the equation of motion of BO equation, and $\dot{\Phi}_S$ and $\dot{\Psi}_S$ are obtained through perturbation equations.

It is convenient to study the motion of a binary system in such a coordinate system (J-coordinate system), in which the total angular momentum, \mathbf{J} is along the z-axis and the invariance plane is in the x-y plane. J-coordinate system has two advantages.

(a) Once a binary pulsar system is given, the misalignment angle between \mathbf{J} and \mathbf{L} , λ_{LJ} is determined, from which $\dot{\Phi}_S$ (or $\dot{\Omega}$) and $\dot{\Psi}_S$ (or $\dot{\omega}$) can be obtained easily in J-coordinate system, which are intrinsic to a binary pulsar system.

(b) Moreover, J-coordinate system is static relative to the line of sight (after counting out the proper motion). Therefore transforming the secular parameters obtained J-coordinates system to observer's coordinate system, S-L coupling induced effects can be obtain reliably.

From Eq(2), we have,

$$V = V_1 + V_2 = \frac{1}{r^3} (2\mathbf{S} + \frac{3m_2}{2m_1}\mathbf{S}_1 + \frac{3m_1}{2m_2}\mathbf{S}_2) \cdot \mathbf{L}, \quad (35)$$

which can be written as,

$$V = \frac{1}{r^3} (\sigma_1 \mathbf{S} \cdot \mathbf{L} + \sigma_2 \mathbf{S}_2 \cdot \mathbf{L}), \quad (36)$$

where

$$\sigma_1 = 2 + \frac{3m_2}{2m_1}, \quad \sigma_2 = 2 + \frac{3}{2} \left(\frac{m_1}{m_2} - \frac{m_2}{m_1} \right). \quad (37)$$

The acceleration is given,

$$\mathbf{a}_{so} = -\nabla V = -\sigma_1 \nabla \frac{(\mathbf{S} \cdot \mathbf{L})}{r^3} - \sigma_2 \nabla \frac{(\mathbf{S}_2 \cdot \mathbf{L})}{r^3}. \quad (38)$$

Once the triangle constraint ($\mathbf{J} = \mathbf{S} + \mathbf{L}$) is satisfied then the first term at the right hand side of Eq(38) can be written,

$$\nabla \frac{(\mathbf{S} \cdot \mathbf{L})}{r^3} = \nabla \frac{[(\mathbf{J} - \mathbf{L}) \cdot \mathbf{L}]}{r^3} = \nabla \frac{(\mathbf{J} \cdot \mathbf{L})}{r^3} - \nabla \frac{(\mathbf{L} \cdot \mathbf{L})}{r^3}. \quad (39)$$

where

$$\nabla \frac{(\mathbf{J} \cdot \mathbf{L})}{r^3} = -3 \frac{(\mathbf{L} \cdot \mathbf{J})\mathbf{r}}{r^5} - 3 \frac{(\mathbf{J} \times \mathbf{r})(\mathbf{V} \cdot \mathbf{r})}{r^5} + 2 \frac{(\mathbf{J} \times \mathbf{V})}{r^3} \quad (40)$$

$$\nabla \frac{(\mathbf{L} \cdot \mathbf{L})}{r^3} = -3 \frac{(\mathbf{L} \cdot \mathbf{L})\mathbf{r}}{r^5} - 3 \frac{(\mathbf{L} \times \mathbf{r})(\mathbf{V} \cdot \mathbf{r})}{r^5} + \frac{(\mathbf{L} \times \mathbf{V})}{r^3} \quad (41)$$

Notice that the coefficient of the third term at the right hand side of Eq(40) and Eq(41) are different, the reason is that \mathbf{J} is a not a function of r , whereas \mathbf{L} is. Put Eq(40) and Eq(41) into Eq(39) and finally into Eq(38), we have,

$$\begin{aligned} \mathbf{a}_{so} = & \frac{3}{r^3} [\sigma_1 \mathbf{S} \cdot (\hat{\mathbf{n}} \times \mathbf{V}) \hat{\mathbf{n}} + \sigma_2 \mathbf{S}_2 \cdot (\hat{\mathbf{n}} \times \mathbf{V}) \hat{\mathbf{n}}] \\ & + \frac{1}{r^3} [\sigma_1 (\mathbf{V} \times \mathbf{J}) + \sigma_1 (\mathbf{V} \times \mathbf{S}) + 2\sigma_2 (\mathbf{V} \times \mathbf{S}_2)] \\ & + \frac{3(\mathbf{V} \cdot \hat{\mathbf{n}})}{r^3} [\sigma_1 (\mathbf{S} \times \hat{\mathbf{n}}) + \sigma_2 (\mathbf{S}_2 \times \hat{\mathbf{n}})]. \end{aligned} \quad (42)$$

Obviously all terms at the right hand side of Eq(42) are 1.5PN except the term containing \mathbf{J} , which is caused by the triangle constraint given by Eq(39)–Eq(41). If one calculates \mathbf{a}_{so} directly by Eq(38) without imposing the triangle constraint, then the corresponding result can be given by replacing \mathbf{J} of Eq(42) by \mathbf{S} ,

$$\begin{aligned} \mathbf{a}'_{so} = & \frac{3}{r^3} [\sigma_1 \mathbf{S} \cdot (\hat{\mathbf{n}} \times \mathbf{V}) \hat{\mathbf{n}} + \sigma_2 \mathbf{S}_2 \cdot (\hat{\mathbf{n}} \times \mathbf{V}) \hat{\mathbf{n}}] \\ & + \frac{2}{r^3} [\sigma_1 (\mathbf{V} \times \mathbf{S}) + \sigma_2 (\mathbf{V} \times \mathbf{S}_2)] \\ & + \frac{3(\mathbf{V} \cdot \hat{\mathbf{n}})}{r^3} [\sigma_1 (\mathbf{S} \times \hat{\mathbf{n}}) + \sigma_2 (\mathbf{S}_2 \times \hat{\mathbf{n}})]. \end{aligned} \quad (43)$$

Notice that Eq(43) is equivalent to the sum of Eq(52) and Eq(53) given by BO equation[1]. The difference between Eq(42) and Eq(43) indicates that whether the triangle constraint is imposed or not can lead to significant differences in \mathbf{a}_{so} , which in turn results significant differences

on the predictions of observational effects as discussed in the rest of this section.

In Eq(42) $\hat{\mathbf{n}}$ is the unit vector of \mathbf{r} , which is given by,

$$\hat{\mathbf{n}} = \mathbf{P} \cos f + \mathbf{Q} \sin f , \quad (44)$$

and $\hat{\mathbf{t}}$ is the unit vector that is perpendicular to $\hat{\mathbf{n}}$,

$$\hat{\mathbf{t}} = -\mathbf{P} \sin f + \mathbf{Q} \cos f , \quad (45)$$

and $\mathbf{V} = \mathbf{p}/\mu$, is given by

$$\mathbf{V} = -\frac{h}{p}\mathbf{P} \cos f + \frac{h}{p}\mathbf{Q}(e + \cos f) , \quad (46)$$

where f is the true anomaly, p is the semilatus rectum, $p = a(1 - e^2)$, and h is the integral of area, $h = r^2 \dot{f}$. \mathbf{P} is given by three components,

$$P_x = \cos \Omega \cos \omega - \sin \Omega \sin \omega \cos \lambda_{LJ} ,$$

$$P_y = \sin \Omega \cos \omega + \cos \Omega \sin \omega \cos \lambda_{LJ} ,$$

$$P_z = \sin \omega \sin \lambda_{LJ} , \quad (47)$$

and \mathbf{Q} is given by three components,

$$Q_x = -\cos \Omega \sin \omega - \sin \Omega \cos \omega \cos \lambda_{LJ} ,$$

$$Q_y = -\sin \Omega \sin \omega + \cos \Omega \cos \omega \cos \lambda_{LJ} ,$$

$$Q_z = \cos \omega \sin \lambda_{LJ} , \quad (48)$$

The unit vector of $\hat{\mathbf{L}}$ and $\hat{\mathbf{S}}_\kappa$ ($\kappa = 1, 2$) are given,

$$\hat{\mathbf{L}} = (\sin \lambda_{LJ} \cos \eta_L, \sin \lambda_{LJ} \sin \eta_L, \cos \lambda_{LJ}) , \quad (49)$$

$$\hat{\mathbf{S}}_\kappa = (\sin \lambda_{JS\kappa} \cos \eta_{S\kappa}, \sin \lambda_{JS\kappa} \sin \eta_{S\kappa}, \cos \lambda_{JS\kappa}) . \quad (50)$$

In perturbation equation, the acceleration of Eq(42), \mathbf{a}_{so} , is expressed along $\hat{\mathbf{n}}$, $\hat{\mathbf{t}}$ and $\hat{\mathbf{L}}$ respectively. We can use \mathbf{a}_1 , \mathbf{a}_2 and \mathbf{a}_3 to represent terms corresponding to the three brackets [,] at the right hand side of Eq(42) respectively. Projecting \mathbf{a}_1 to $\hat{\mathbf{L}}$, we have,

$$W_1 = \mathbf{a}_1 \cdot \hat{\mathbf{L}} = \frac{3\sigma_1}{r^3} [S_x(n_y V_z - n_z V_y)$$

$$+ S_y(n_z V_x - n_x V_z) + S_z(n_z V_y - n_y V_z)]$$

$$(n_x \sin \lambda_{LJ} \cos \eta_L + n_y \sin \lambda_{LJ} \sin \eta_L + n_z \cos \lambda_{LJ}) \quad (51)$$

where n_x, n_y, n_z and V_x, V_y, V_z are components of $\hat{\mathbf{n}}$ and \mathbf{V} along axes, x, y and z respectively. Similarly, projecting \mathbf{a}_2 to $\hat{\mathbf{L}}$, we have,

$$W_2 = \mathbf{a}_2 \cdot \hat{\mathbf{L}} = \frac{\sigma_1}{r^3} (V_y J \sin \lambda_{LJ} \cos \eta_L - V_x J \sin \lambda_{LJ} \sin \eta_L)$$

$$+ [\frac{\sigma_1}{r^3} (V_x S_y - V_y S_x) + \frac{2\sigma_2}{r^3} (V_x S_{2y} - V_y S_{2x})] \cos \lambda_{LJ} \quad (52)$$

Similarly \mathbf{a}_3 can also be projected to $\hat{\mathbf{L}}$,

$$W_3 = \mathbf{a}_3 \cdot \hat{\mathbf{L}} = \frac{1}{r^3} [\sigma_1 (V_y^r S \sin \lambda_{LJ} \cos \eta_L$$

$$- V_x^r S \sin \lambda_{LJ} \sin \eta_L) + \sigma_2 (V_x^r S_{2y} - V_y^r S_{2x})] \quad (53)$$

where $V_x^r = 3\dot{r}n_x$ and $V_y^r = 3\dot{r}n_y$. Therefore, the sum of W is

$$W = W_1 + W_2 + W_3 \quad (54)$$

The effect around \mathbf{J} can be obtained by perturbation equations[11, 12, 13] and Eq(54)

$$\frac{d\Omega}{dt} = \frac{Wr \sin(\omega + f)}{na^2 \sqrt{1 - e^2}} \frac{1}{\sin \lambda_{LJ}} , \quad (55)$$

where n is the angular velocity. Average over one orbital period we have,

$$\langle \frac{d\Omega}{dt} \rangle = \frac{3 \cos \lambda_{LJ}}{2a^3 (1 - e^2)^{3/2} \sin \lambda_{LJ}} (P_z \sin \omega + Q_x \cos \omega)$$

$$[(P_y Q_z - P_z Q_y)(S_x \sigma_1 + S_{2x} \sigma_2)$$

$$+ (P_z Q_z - P_x Q_x)(S_y \sigma_1 + S_{2y} \sigma_2)$$

$$+ (P_x Q_y - P_y Q_x)(S_z \sigma_1 + S_{2z} \sigma_2)] . \quad (56)$$

Notice that the average value of Eq(56) depends only on W_1 , the contribution of W_2 and W_3 to it is zero. With $S/\sin \lambda_{LJ} \sim L$, we have $\frac{d\Omega}{dt} \sim \frac{3L}{2a^3}$, which corresponds to 1PN.

The $d\omega/dt$ can be obtained by calculation of $\tilde{S} = \mathbf{a}_{SO} \cdot \hat{\mathbf{n}}$ and $T = \mathbf{a}_{SO} \cdot \hat{\mathbf{t}}$. Since $\mathbf{a}_1 \cdot \hat{\mathbf{n}}$, $\mathbf{a}_1 \cdot \hat{\mathbf{t}}$, $\mathbf{a}_3 \cdot \hat{\mathbf{n}}$ and $\mathbf{a}_3 \cdot \hat{\mathbf{t}}$ are 1.5PN, which are negligible in the discussion of 1PN, therefore, it is sufficient to consider the projection of \mathbf{a}_2 to $\hat{\mathbf{n}}$, $\hat{\mathbf{t}}$ respectively. And since that only the first term of \mathbf{a}_2 , as shown in Eq(38), is 1PN, the other two terms are 1.5PN, which are negligible in the discussion of 1PN, thus we have,

$$\langle (\mathbf{a}_2 \cdot \hat{\mathbf{n}}) \cos f \rangle = \frac{\sigma_1 J}{2(1 - e^2)^{3/2} a^3} \frac{eh}{p} (P_x Q_y - P_y Q_x) , \quad (57)$$

$$\langle (\mathbf{a}_2 \cdot \hat{\mathbf{t}}) \sin f \rangle = \frac{-\sigma_1 J}{2(1-e^2)^{3/2} a^3} \frac{eh}{p} (P_x Q_y - P_y Q_x) , \quad (58)$$

By Eq(57) and Eq(58), the S-L coupling induced $d\omega/dt$ is given[11, 12, 13],

$$\frac{d\omega'}{dt} = \frac{\sqrt{1-e^2}}{nae} \{ [-\mathbf{a}_2 \cdot \hat{\mathbf{n}}] \cos f + (1 + \frac{r}{p}) [\mathbf{a}_2 \cdot \hat{\mathbf{t}}] \sin f \} . \quad (59)$$

therefore, by the standard perturbation, the advance of precession of periastron, which corresponds to Eq(28) of Apostolatos et al[6], is given,

$$\frac{d\omega}{dt} = \frac{d\omega'}{dt} - \frac{d\Omega}{dt} \cos \lambda_{LJ} . \quad (60)$$

By putting Eq(57) and Eq(58) into Eq(60), and average over one orbital period we have,

$$\langle \frac{d\omega}{dt} \rangle = \frac{3\sigma_1 J}{2(1-e^2)^{3/2} a^3} (P_x Q_y - P_y Q_x) - \frac{d\Omega}{dt} \cos \lambda_{LJ} . \quad (61)$$

Using perturbation equations[11, 12, 13], and by Eq(55) and Eq(61), we have,

$$\begin{aligned} \langle \frac{d\omega^S}{dt} \rangle &= \frac{3\sigma_1 J}{2(1-e^2)^{3/2} a^3} (P_x Q_y - P_y Q_x) + 2 \frac{d\Omega}{dt} \sin^2 \frac{\lambda_{LJ}}{2} \\ &= \frac{3\sigma_1 J}{2(1-e^2)^{3/2} a^3} (P_x Q_y - P_y Q_x) + O(c^{-5}) . \end{aligned} \quad (62)$$

Eq(56), Eq(61) and Eq(62) indict that the magnitude of $\frac{d\Omega}{dt}$, and $\frac{d\omega^S}{dt}$ are both $\frac{3L}{2a^3}$ (1PN), whereas, $\frac{d\omega}{dt}$ can be 1.5PN, in the sense that $\frac{d\omega}{dt} \sim (\frac{3J}{2a^3} - \frac{3L}{2a^3})$, as shown in Eq(61). Therefore, $\frac{d\omega}{dt}$ can be consistent with Apostolatos et al[6]'s result.

$\frac{d\Omega}{dt}$ (1PN) of Eq(55) is equivalent to $\dot{\Phi}$ (1PN) of Eq(30) which is given by Wex and Kopeikin [5]. This is because the averaged value of $\frac{d\Omega}{dt}$ depends only on \mathbf{a}_1 , the first bracket [,] of \mathbf{a}_{so} , as shown in Eq(42). And both this paper (\mathbf{a}_{so} of Eq(42)) and that of BO equation (\mathbf{a}'_{so} of Eq(43)) give the same \mathbf{a}_1 . Thus, different authors give the equivalent value on the averaged $\frac{d\Omega}{dt}$.

Whereas, $\frac{d\omega}{dt}$ (1.5PN) of Eq(61) and $\dot{\Psi}$ (1PN) of Eq(31) are very different in magnitude, and thus $\frac{d\omega^S}{dt}$ predicted by this paper and that of Wex and Kopeikin are also very different. The difference is due to that $\frac{d\omega}{dt}$ and $\frac{d\omega^S}{dt}$ given by Eq(61) and Eq(62) of this paper are obtained by the \mathbf{a}_{so} of Eq(42), whereas, the corresponding $\frac{d\omega}{dt}$ and $\frac{d\omega^S}{dt}$ of Wex and Kopeikin (which is equivalent of replacing J of Eq(61) and Eq(62) by S) are obtained by the \mathbf{a}'_{so} of Eq(43).

And in turn, the difference between \mathbf{a}_{so} and \mathbf{a}'_{so} is due to that \mathbf{a}_{so} includes the triangle constraints whereas, \mathbf{a}'_{so} doesn't. Therefore, a small difference in the equation of

motion causes significant discrepancy in the variation of elements, $\frac{d\omega}{dt}$ and $\frac{d\omega^S}{dt}$, which in turn corresponding to significant discrepancy on the prediction of observational effects.

V. EFFECTS ON $\dot{\omega}$, \dot{x} , \dot{P}_b

Whether the definition of \mathbf{J} is satisfied or not, corresponds to very different magnitude on $\dot{\Omega}$ and $\dot{\omega}$, and in turn corresponds to very different effects on the secular parameters, such as $\dot{\omega}$, \dot{x} , \dot{P}_b .

The relationship of Ω , the longitude of periastron, ω , and the orbital inclination, i , can be given by [3, 5]

$$\cos i = \cos I \cos \lambda_{LJ} - \sin \lambda_{LJ} \sin I \cos \Omega , \quad (63)$$

and

$$\begin{aligned} \sin i \sin \omega^{obs} &= (\cos I \sin \lambda_{LJ} + \cos \lambda_{LJ} \sin I \cos \Omega) \sin \omega \\ &+ \sin I \sin \Omega \cos \omega , \end{aligned} \quad (64)$$

$$\begin{aligned} \sin i \cos \omega^{obs} &= (\cos I \sin \lambda_{LJ} + \cos \lambda_{LJ} \sin I \cos \Omega) \cos \omega \\ &- \sin I \sin \Omega \sin \omega , \end{aligned} \quad (65)$$

where I is the misalignment angle between \mathbf{J} and line of sight. The semi-major axis of the pulsar is defined as

$$x \equiv \frac{a_p \sin i}{c} . \quad (66)$$

where a_p is the semi-major axes of the pulsar. By Eq(63), we have,

$$\dot{x}_1 = \frac{a_p \cos i}{c} \frac{di}{dt} = -x \dot{\Omega} \sin \lambda_{LJ} \sin \Omega \cot i . \quad (67)$$

The semi-major axes of the orbit is $a = \frac{M}{m_2} a_p$, and since the L-S coupling induced \dot{a} is a function of Ω and ω , as shown in appendix, we have

$$\dot{x}_2 = \frac{\dot{a}_p \sin i}{c} = \frac{\dot{a}}{a} x . \quad (68)$$

Therefore, the L-S coupling induced \dot{x} is given,

$$\dot{x} = \dot{x}_1 + \dot{x}_2 = -x \dot{\Omega} \sin \lambda_{LJ} \sin \Omega \cot i + \frac{\dot{a}}{a} x . \quad (69)$$

By Eq(69) we have,

$$\ddot{x} = \dot{x}_1 (\dot{\Omega}/\dot{\Omega} + \dot{\Omega} \cot \Omega) + x \frac{\ddot{a}a - \dot{a}^2}{a^2} + \dot{x}_2 \frac{\dot{a}}{a} . \quad (70)$$

Notice that $\dot{\Omega}$ and $d^2\Omega/dt^2$ can be obtained by Eq(55).

Considering $\lambda_{LJ} \ll 1$ and by Eq(64), Eq(65), the observational advance of precession of periastron is given [3, 5]

$$\omega^{obs} = \omega + \Omega - \lambda_{LJ} \cot i \sin \Omega . \quad (71)$$

Therefore, we have,

$$\dot{\omega}^{obs} = \dot{\omega} + \dot{\Omega} - \lambda_{LJ} \dot{\Omega} \cot i \cos \Omega . \quad (72)$$

If $\dot{\omega}$ and $\dot{\Omega}$ are only caused by the S-L coupling effect ($H = H_S$), then $\dot{\omega} + \dot{\Omega} = \frac{d\omega^S}{dt}$, where $\frac{d\omega^S}{dt}$ is given by Eq(62). If we consider all terms of Hamiltonian, as given by Eq(1), then $\dot{\omega}$ should include the contribution by H_{1PN} , which causes $\dot{\omega}^{GR}$, the advance of precession of periastron predicted by general relativity. In such case $\dot{\omega}$ in Eq(72) is replaced by $\dot{\omega}' = \dot{\omega}^{GR} + \dot{\omega}$. Thus Eq(72) can be written as,

$$\dot{\omega}^{obs} = \dot{\omega}^{GR} + \dot{\omega}^S + O(c^{-5}) . \quad (73)$$

Notice that the third term at the right hand side of Eq(72) is ignorable in 1PN. $\dot{\omega}^S$ is a function of time as shown in Eq(62), whereas, $\dot{\omega}^{GR}$ is a constant as shown in Eq(9).

For a binary pulsar system with negligibly small eccentricity, the effect of the secular variation in the advance of periastron, ω , is absorbed by the redefinition of the orbital frequency. As discussed by Kopeikin [9], $\omega^{obs} + A_e(u)$ is given

$$\omega^{obs} + A_e(u) = \omega_0 + \frac{2\pi}{P_b}(t - t_0) , \quad (74)$$

where $A_e(u)$ is the true anomaly, related to the eccentric anomaly, u , by the well-known transcendental equation, ω_0 is the orbital phase at the initial epoch t_0 .

In Eq(74) P_b is treated as a constant. By assuming that $\delta t = (t - t_0)$ is a small value, Eq(74) can also be applied to the case that P_b is a function of time. Then we have

$$\delta\omega^{obs} + A_e(u) = \frac{2\pi}{P_b}\delta t , \quad (75)$$

The first derivative of Eq(75) gives,

$$\delta\dot{\omega}^{obs} + \dot{A}_e(u) = \frac{2\pi}{P_b} + \left(\frac{2\pi}{P_b}\right)'\delta t , \quad (76)$$

by $\dot{A}_e(u) = \frac{2\pi}{P_b}$, we have

$$\delta\dot{\omega}^{obs} = -\frac{2\pi\dot{P}_b}{P_b^2}\delta t . \quad (77)$$

Since $\dot{\omega}^S$ is a function of time, whereas $\dot{\omega}^{GR} = const$, then we have $\dot{\omega}^{obs} = \dot{\omega}^S$ by Eq(73). Assume $F = \dot{\omega}^S$, and by $F = F_0 + \dot{F}\delta t + \frac{1}{2}\ddot{F}\delta t^2$, we have $\delta F = \delta\dot{\omega}^S \approx \dot{F}\delta t = \dot{\omega}^S\delta t$. Therefore, the left hand side of Eq(77)

becomes $\delta\dot{\omega}^S = \dot{\omega}^S\delta t$, from which Eq(77) can be written as,

$$\dot{P}_b = -\frac{\dot{\omega}^S P_b^2}{2\pi} . \quad (78)$$

By Eq(78), the derivatives of P_b can be obtained,

$$\ddot{P}_b = \frac{2\dot{P}_b^2}{P_b} - \frac{\ddot{\omega}^S P_b^2}{2\pi} \approx -\frac{\dot{\omega}^S P_b^2}{2\pi} , \quad (79)$$

$$\ddot{P}_b \approx -\frac{P_b^2}{2\pi} \frac{d^4\omega^S}{dt^4} . \quad (80)$$

Since $\frac{d\Omega}{dt}$ ($\dot{\Phi}_S$) given by Wex and Kopeikin's [5] is equivalent to that of Eq(55), thus \dot{x} and \ddot{x} given by Wex and Kopeikin and this paper are equivalent in the case that only S-L coupling effect is considered.

In Wex and Kopeikin's treatment of observational effects, Eq(69) and Eq(72), BO's orbital precession velocity, $\dot{\Omega}_S$ is decomposed to \mathbf{L} and \mathbf{J} , which is equivalent to be transformed into J-coordinate system. And therefore, parameters are transformed from J-coordinate system to line of sight. If BO's orbital precession velocity, $\dot{\Omega}_S$ is replaced by AK's $\dot{\Omega}_0$ then this treatment could predict correct effects.

Brumberg's equation is similar to BO's equation, in which \mathbf{L} is treated as precession around an instantaneous axes, which violates the triangle constraint.

The treatment of this paper is imposing the triangle constraint to the equation of motion of BO, and obtains effects in J-coordinate system, and then transform to the line of sight, as shown in Table I and Table II.

VI. CONFRONTATION WITH OBSERVATION

The precise secular parameters measured in some binary pulsars provides chance to test the two kinds of predictions. $\dot{\Omega}$ given by Wex and Kopeikin's [5] can explain \dot{x} , however the corresponding $\dot{\omega}$ cannot explain significant \dot{P}_b measured. The effects predicted by this paper can explain both \dot{x} and \dot{P}_b measured in the four binary pulsars.

A. PSR J2051-0827

By Eq(69), we have

$$\dot{\Omega} = -\frac{\dot{x}}{x} \frac{\tan i}{\sin \lambda_{LJ} \sin \Omega_0} = -\frac{di}{dt} \frac{1}{\sin \lambda_{LJ} \sin \Omega_0} . \quad (81)$$

According to optical observations, the system is likely to be moderately inclined with an inclination angle $i \sim 40^\circ$ [14]. By the measured results of $x = 0.045s$, $\dot{x} = -23(3) \times$

10^{-14} [15], and by assuming $\sin \lambda_{LJ} \sin \Omega_0 = 2 \times 10^{-3}$, Eq(81) can be written in magnitude,

$$\dot{\Omega} = \left(\frac{\dot{x}}{2.3 \times 10^{-13}}\right) \left(\frac{x}{0.045}\right)^{-1} \left(\frac{\tan i}{\tan 40^\circ}\right) \left(\frac{\sin \lambda_{LJ} \sin \Omega_0}{2 \times 10^{-3}}\right)^{-1} \\ \sim 2 \times 10^{-9} (s^{-1}) . \quad (82)$$

And by Eq(61), we can assume $\ddot{\omega}^S \sim (\dot{\omega}^S)^2 \sim c_1 \dot{\Omega}^2 \approx 4 \times 10^{-18}$ ($c_1 = 1$). Thus by Eq(78),

$$\dot{P}_b = \frac{1}{2\pi} \left(\frac{\dot{\omega}^S}{4 \times 10^{-18}}\right) \left(\frac{P_b}{0.099d}\right)^2 \sim 5 \times 10^{-11} s s^{-1} . \quad (83)$$

By Eq(62), we can see that $\ddot{\omega}^S$, $\ddot{\omega}^S$ and $d^4 \omega^S / dt^4$ can vary in different range, which can be written approximately as (for the convenience of estimation),

$$|\dot{\omega}^S| \approx c_1 \dot{\Omega}^2 , \quad |\ddot{\omega}^S| \approx c_2 \dot{\Omega}^3 , \quad \left|\frac{d^4 \omega^S}{dt^4}\right| \approx c_3 \dot{\Omega}^4 , \quad (84)$$

Obviously $\frac{d^4 \omega^S}{dt^4}$ can vary in a wider range than $\ddot{\omega}^S$, and $\ddot{\omega}^S$ can vary in a wider range than $\dot{\omega}^S$.

By Eq(84), we can estimate $\ddot{\omega}^S \sim c_2 \dot{\Omega}^3 \approx 8 \times 10^{-27} s^{-3}$ ($c_2 = 1$), similarly, we can estimate $d^4 \omega^S / dt^4 \sim c_3 \dot{\Omega}^4 \approx 16 \times 10^{-36} s^{-4}$ ($c_3 = 1$).

Therefore, by Eq(79) and Eq(80) we have $\ddot{P}_b \sim 9 \times 10^{-20} s^{-1}$ and $\ddot{P}_b \sim 2 \times 10^{-28} s^{-2}$. By Eq(69) and Eq(70), $\ddot{x}/\dot{x} \sim \dot{\Omega} \sim 2 \times 10^{-9} s^{-1}$, which can well consistent with observation as shown in Table III.

Therefore, once \dot{x} is satisfied with observation, the corresponding $\dot{\omega}^S$ can make the derivatives of P_b consistent with observation as shown in Table III. Whereas, the effect derived from Wex and Kopeikin's equation can only be consistent with \dot{x} , the significant derivatives of P_b cannot be explained.

B. PSR B1957+20

Similarly, by the measured parameters, $x = 0.089s$, $|\dot{x}| < 3 \times 10^{-14}$ [16], and assuming, $i = 45^\circ$, $\sin \lambda_{LJ} \sin \Omega_0 = 1 \times 10^{-3}$, we have,

$$\dot{\Omega} = \left(\frac{\dot{x}}{3 \times 10^{-14}}\right) \left(\frac{x}{0.089}\right)^{-1} \left(\frac{\tan i}{\tan 45^\circ}\right) \left(\frac{\sin \lambda_{LJ} \sin \Omega_0}{1 \times 10^{-3}}\right)^{-1} \\ \sim 3 \times 10^{-10} (s^{-1}) . \quad (85)$$

Similarly, we can assume $\ddot{\omega}^S \sim c_1 \dot{\Omega}^2 \approx 4 \times 10^{-18} s^{-2}$ ($c_1 = 1$). Similarly \dot{P}_b is given,

$$\dot{P}_b = \frac{1}{2\pi} \left(\frac{\dot{\omega}^S}{9 \times 10^{-20}}\right) \left(\frac{P_b}{33002}\right)^2 \sim 2 \times 10^{-11} s s^{-1} . \quad (86)$$

And similar as PSR 201-0827, we can estimate $\ddot{\omega}^S \sim c_2 \dot{\Omega}^3 \approx 27 \times 10^{-28} s^{-3}$ ($c_2 = 10^2$), $d^4 \omega^S / dt^4 \sim c_3 \dot{\Omega}^4 \approx$

$81 \times 10^{-36} s^{-4}$ ($c_3 = 10^4$). Therefore, by Eq(79) and Eq(80) we have $\dot{P}_b \sim 5 \times 10^{-19} s^{-1}$ and $\ddot{P}_b \sim 1 \times 10^{-26} s^{-2}$, as shown in Table IV.

The different magnitude of c_1 , c_2 and c_3 in PSR B1957+20 and PSR J2051-0827 means that the angles of the three vectors, \mathbf{S}_1 , \mathbf{S}_2 and \mathbf{L} , the masses and spin angular momenta of the two stars in these two binary pulsars are different.

C. PSR J1012+5307

By the measured parameters, $x = 0.58s$, $|\dot{x}| < 1.4 \times 10^{-14}$, $i = 52^\circ$ [17], and by assuming $\sin \lambda_{LJ} \sin \Omega_0 = 1 \times 10^{-3}$, then $\dot{\Omega}$ is given,

$$\dot{\Omega} = \left(\frac{\dot{x}}{1.4 \times 10^{-14}}\right) \left(\frac{x}{0.58}\right)^{-1} \left(\frac{\tan i}{\tan 52^\circ}\right) \left(\frac{\sin \lambda_{LJ} \sin \Omega_0}{1 \times 10^{-3}}\right)^{-1} \\ \sim 3 \times 10^{-11} (s^{-1}) , \quad (87)$$

similarly with $c_1 = 1$, \dot{P}_b can be obtained,

$$\dot{P}_b = \frac{1}{2\pi} \left(\frac{\dot{\omega}^S}{9 \times 10^{-22}}\right) \left(\frac{P_b}{0.6d}\right)^2 \sim 4 \times 10^{-13} s s^{-1} . \quad (88)$$

The comparison of observational and predicted secular variabilities are shown Table V, which indicts that they can be consistent.

D. PSR J1713+0747

By the measured parameters, $x = 32.3s$, $|\dot{x}| = 5(12) \times 10^{-15}$, $i = 70^\circ$ [18], and by assuming $\sin \lambda_{LJ} \sin \Omega_0 = 1 \times 10^{-4}$, then in magnitude we have,

$$\dot{\Omega} = \left(\frac{\dot{x}}{5 \times 10^{-15}}\right) \left(\frac{x}{32.3}\right)^{-1} \left(\frac{\tan i}{\tan 70^\circ}\right) \left(\frac{\sin \lambda_{LJ} \sin \Omega_0}{1 \times 10^{-4}}\right)^{-1} \\ \sim 4 \times 10^{-12} (s^{-1}) , \quad (89)$$

similarly with $c_1 = 1$ we have,

$$\dot{P}_b = \frac{1}{2\pi} \left(\frac{\dot{\omega}^S}{16 \times 10^{-26}}\right) \left(\frac{P_b}{67.8d}\right)^2 \sim 1 \times 10^{-10} s s^{-1} . \quad (90)$$

The comparison of observational and predicted secular variabilities are shown Table VI, which indicts that they can be consistent.

E. discussion

Therefore, the significant \dot{P}_b^{obs} is a natural results of the S-L coupling effect if the triangle constraint is imposed on BO's equation of motion.

In the case that the triangle constraint is not imposed on the BO equation, the contribution of S-L coupling to the advance of precession of periastron relative to the line of sight is insignificant. And in turn the S-L coupling's contribution to \dot{P}_b is also insignificant, as shown in Eq(78). And since the gravitational radiation induced \dot{P}_b^{GR} is much smaller than that of the measured one, \dot{P}_b^{obs} , thus Wex and kopeikin's equation cannot explain the significant \dot{P}_b^{obs} .

Applegate and Shaham [19] proposed a model to explain the significant \dot{P}_b^{obs} . Their model assumes a variable quadrupole moment which is due to the cyclic spin-up and spin-down of the outer layers of the companion. In which \dot{P}_b^{obs} of binary pulsars like PSR B1957+20 and PSR J2051-0827 can be explained. However this model is not easy to explain higher derivatives like, \ddot{P}_b , $\ddot{\dot{P}}_b$ of these binary pulsars. Moreover it is also not easy to explain binary pulsars with much larger orbital period, i.e., PSR J1713+0747 ($P_b = 67.8\text{day}$), while these phenomena can be well explain by S-L coupling induced effect in the case that the triangle constraint is imposed.

VII. CONCLUSION

Starting from the same relativistic Hamiltonian, Eq(2), and precession of spins Eq(3), one can obtain secular variabilities by different means, as shown in Table I, and the results are different significantly in magnitude, as shown in Table II. The discrepancy is due to the triangle constraint, the calculation without the constraint leads to insignificant parameters i.e., $\dot{\omega}^{obs}$ and \dot{P}_b ; whereas, the calculation with the constraint leads to significant $\dot{\omega}^{obs}$ and \dot{P}_b , as shown in Table II.

BO's orbital precession velocity is expressed as precession around an instantaneous axes, and the corresponding magnitude is 1.5PN, whereas, Apostolatos et al give the orbital precession velocity as precession around a fixed axes, and magnitude is 1PN. And decomposing BO and Apostolatos et al's orbital precession velocities, one can obtain the same component along \mathbf{J} , but very different component along \mathbf{L} . The discrepancy of the components along \mathbf{L} is the result of the discrepancy in the derivation of orbital precession by the two manners. BO's orbital precession velocity is obtained by assuming the orbital angular momentum vector, \mathbf{L} , precessing at equivalent velocity as that of the Runge-Lenz vector, \mathbf{A} , which lead to the violation of BO's orbital precession velocity to the definition of \mathbf{J} ; whereas, AK's orbital precession velocity is obtained without the Runge-Lenz vector, and it can be consistent with the definition of \mathbf{J} . The theory independent result on the component along \mathbf{L} [6], and the observations of secular variabilities do not support BO's orbital precession velocity.

Whereas, component of orbital precession velocity along \mathbf{L} obtained by imposing the triangle constraint on the equation of motion of this paper can be consistent both with the theory independent result on the compo-

nent along \mathbf{L} [6], and the observations of pulsar timing measurement.

Acknowledgments

I thank T.Huang for help in clarifying the theoretical part of this paper. I thank R.N. Manchester for his help in understanding pulsar timing measurement. I thank T. Lu for useful comments during this work. I thank W.T. Ni and C.M. Xu for useful suggestions in the presentation of this paper. I thank E.K.Hu, A.Rüdiger, K.S.Cheng, N.S.Zhong, and Z.G.Dai for continuous encouragement and help. I also thank Z.X. Yu, C.M. Zhang, L. Zhang, Z.Li, H. Zhang, S.Y.Liu, X.N.Lou, X.S.Wan for useful discussion.

VIII. APPENDIX

By $\tilde{S} = \mathbf{a}_{SO} \cdot \hat{\mathbf{n}}$ and $T = \mathbf{a}_{SO} \cdot \hat{\mathbf{t}}$, $\frac{d\Omega}{dt}$ and $\frac{d\omega}{dt}$ have been given by Eq(55), Eq(56), Eq(59), and Eq(61), following the standard procedure for computing perturbations of orbital elements [11]. Similiarly, four other elements can be given,

$$\frac{da}{dt} = \frac{2}{n\sqrt{1-e^2}}(\tilde{S}e \sin f + \frac{pT}{r}) , \quad (91)$$

$$\begin{aligned} \langle \frac{da}{dt} \rangle &= \frac{\sigma_1 J e^2}{4n(1-e^2)^2 a^3} (P_x Q_y - P_y Q_x) \\ &+ \frac{\sigma_1 J}{(1-e^2)^{5/2} a^2} (P_x Q_y - P_y Q_x) (1 + \frac{3}{4}e) , \end{aligned} \quad (92)$$

$$\frac{de}{dt} = \frac{\sqrt{1-e^2}}{na} [\tilde{S} \sin f + T(\cos E + \cos f)] , \quad (93)$$

$$\langle \frac{de}{dt} \rangle = \frac{\sigma_1 J e}{8(1-e^2)^{3/2} a^3} (P_x Q_y - P_y Q_x) \left[\frac{\sqrt{1-e^2}}{na} + 7 \right] , \quad (94)$$

$$\frac{d\lambda_{LJ}}{dt} = \frac{Wr \cos(\omega + f)}{na^2 \sqrt{1-e^2}} \frac{1}{\sin \lambda_{LJ}} , \quad (95)$$

$$\begin{aligned} \langle \frac{d\lambda_{LJ}}{dt} \rangle &= \frac{3 \cos \lambda_{LJ}}{2a^3 (1-e^2)^{3/2} \sin \lambda_{LJ}} (P_z \cos \omega + Q_x \sin \omega) \\ &[(P_y Q_z - P_z Q_y)(S_x \sigma_1 + S_{2x} \sigma_2) \\ &+ (P_z Q_z - P_x Q_x)(S_y \sigma_1 + S_{2y} \sigma_2)] \end{aligned}$$

$$+(P_x Q_y - P_y Q_x)(S_z \sigma_1 + S_{2z} \sigma_2) , \quad (96)$$

$$\frac{d\epsilon}{dt} = \frac{e^2}{1 + \sqrt{1 - e^2}} \frac{d\omega_S}{dt} + 2 \frac{d\Omega}{dt} (1 - e^2)^{1/2} \left(\sin^2 \frac{\lambda_{LJ}}{2} \right) - \frac{2r\tilde{S}}{na^2} , \quad (97)$$

where $\frac{d\omega_S}{dt} = \frac{d\omega'}{dt} + 2 \frac{d\Omega}{dt} \left(\sin^2 \frac{\lambda_{LJ}}{2} \right)$.

$$\left\langle \frac{d\epsilon}{dt} \right\rangle = \frac{e^2}{1 + \sqrt{1 - e^2}} \left\langle \frac{d\omega_S}{dt} \right\rangle$$

$$+ 2 \left\langle \frac{d\Omega}{dt} \right\rangle (1 - e^2)^{1/2} \left(\sin^2 \frac{\lambda_{LJ}}{2} \right)$$

$$- \frac{1}{n} \frac{\sigma_1 J}{a^4 (1 - e^2)^{1/2}} (P_x Q_y - P_y Q_x) , \quad (98)$$

-
- [1] B.M. Barker, and R.F. O'Connell, Phys. Rev. D, **12**, 329-335 (1975).
- [2] T. Damour and G. Schäfer IL Nuovo Cimento, **101B**, 127 (1988).
- [3] L.L. Smarr, and R.D. Blandford, Astrophys.J. **207**, 574-588 (1976).
- [4] D. Lai, L. Bildsten, and V. Kaspi, Astrophys.J. **452**, 819-824 (1995).
- [5] N. Wex, and S.M. Kopeikin, Astrophys J., **514**, 388 (1999).
- [6] T.A. Apostolatos, C. Cutler, J.J. Sussman, and K.S. Thorne, Phys. Rev. D, **49**, 6274-6297 (1994).
- [7] L.E. Kidder, Phys. Rev. D, **52**, 821-847 (1995).
- [8] Hamilton, A.J.S., and Sarazin, C.L. MNRAS **198**, 59-70 (1982).
- [9] S.M. Kopeikin, Astrophys. J **467**, L93-L95 (1996).
- [10] C.M. Will, Theory and experiment in gravitational physics, Cambridge University Press (1981)
- [11] A.E. Roy, Orbital motion, Adam Hilger (1991)
- [12] Z.H. Yi, Essential Celestial Mechanics, Nanjing University Press (1993)
- [13] L. Liu, Method in Celestial Mechanics, Nanjing University Press (1993)
- [14] B.W. Stappers, M.H. Van Kerkwijk, J.F. Bell, and S.R. Kulkarni, Astrophys. J **548**, L183-L186 (2001).
- [15] O. Doroshenko, O. Löhmer, M. Kramer, A. Jessner, R. Wielebinski, A.G. Lyne, and Ch. Lange, Astro-Astrophys, **379**, 579-588 (2001).
- [16] Z. Arzoumanian, A.S. Fruchter, and J.H. Taylor, Astrophys. J **426**, L85-L88 (1994).
- [17] Ch. Lange, F. Camilo, N. Wex, M. Kramer, D.C. Backer, and A.G. Lyne, MNRAS **326**, 274 (2001).
- [18] F. Camilo, R.S. Foster, and A. Wolszczan, Astrophys. J **437**, L39-L42 (1994).
- [19] J.H. Applegate, and J. Shaham, Astrophys J. **436**, 312-318 (1994).

TABLE I: Comparison of the treatment in obtaining $\dot{\Phi}$ ($\dot{\Omega}$) and $\dot{\Psi}$ ($\dot{\omega}$)

1	$\dot{\mathbf{L}} + \mathbf{A}$	$\rightarrow \dot{\Omega}_S$	$\rightarrow \dot{\Phi}, \dot{\Psi}$
2	$\dot{\mathbf{L}} + \Delta^a$	$\rightarrow \dot{\Omega}_0$	$\rightarrow \dot{\Phi}, \dot{\Psi}$
3	H_S	$\rightarrow \text{EOM}^b + \Delta$	$\rightarrow \dot{\Phi}, \dot{\Psi}$

1. treatment of BO and Wex & Kopeikin, 2. treatment of Apostolatos and this paper, 3. treatment of this paper. ^a Δ represents the triangle constraint. ^b EOM means equation of motion. Notice that 1 correspond to $\dot{\Psi}$ of 1PN, whereas, 2 and 3 correspond to $\dot{\Psi}$ of 1.5PN

TABLE II: Comparison of S-L coupling induced secular variabilities given by different authors

	A	B	evidences
$\dot{\Omega}$ ($\dot{\Phi}$)	1PN	1PN ^a	
$\dot{\omega}$ ($\dot{\Psi}$)	1PN	1.5PN	1.5PN ^b
$\dot{\omega}^S$	1.5PN	1PN	
$\dot{\omega}^{obs}$	$\dot{\omega}^{GR} + 1.5\text{PN}$	$\dot{\omega}^{GR} + 1\text{PN}$	
\dot{P}_b	\dot{P}_b^{GR}	$\dot{P}_b^{GR} - \frac{\dot{\omega}^S P_b^2}{2\pi}$	$\dot{P}_b^{obs} \gg \dot{P}_b^{GRc}$
Δ^d	No	Yes	

A: given by BO [1] and Wex & Kopeikin [5], B: $\dot{\Omega}$ ($\dot{\Phi}$) in one spin case is given by Apostolatos et al [6] and Kidder [7], others are given by this paper. ^a Apostolatos et al [6] and Kidder [7], ^b Apostolatos et al [6], ^c given by [14, 15, 16, 17, 18]. ^d Δ represents the triangle constraint. Notice that except for $\dot{\Omega}$ ($\dot{\Phi}$), all other secular parameters predicted by the two models are different.

TABLE III: Measured parameters compare with the geodetic precession induced ones in PSR J2051–0827

observation	this paper
$\dot{x}^{obs} \approx -23(3) \times 10^{-14}$	$\dot{x} = \dot{x}^{obs}$
$(\ddot{x}/\dot{x})^{obs} \lesssim -3.0 \times 10^{-9} \text{s}^{-1}$	$ \ddot{x}/\dot{x} \approx 2 \times 10^{-9} \text{s}^{-1}$
$\dot{P}_b^{obs} = -15.5(8) \times 10^{-12}$	$ \dot{P}_b = \frac{\dot{\omega}^S P_b^2}{2\pi} \sim 5 \times 10^{-11}$
$\ddot{P}_b^{obs} = 2.1(3) \times 10^{-20} \text{s}^{-1}$	$ \ddot{P}_b = \frac{\ddot{\omega}^S P_b^2}{2\pi} \sim 9 \times 10^{-20} \text{s}^{-1}$
$\ddot{\ddot{P}}_b^{obs} = 3.6(6) \times 10^{-28} \text{s}^{-2}$	$ \ddot{\ddot{P}}_b = \frac{P_b^2}{2\pi} \frac{d^4 \omega^S}{dt^4} \sim 2 \times 10^{-28} \text{s}^{-2}$

In the estimation of parameters in this table, $c_1 = 1$, $c_2 = 1$ and $c_3 = 1$ is assumed.

TABLE IV: Measured parameters compare with the geodetic precession induced ones in PSR B1957+20

observation	this paper
$ \dot{x} ^{obs} < 3 \times 10^{-14}$	$\dot{x} = \dot{x}^{obs}$
$\dot{P}_b^{obs} = 1.47(8) \times 10^{-11}$	$ \dot{P}_b = \frac{\dot{\omega}^S P_b^2}{2\pi} \sim 2 \times 10^{-11}$
$\ddot{P}_b^{obs} = 1.43(8) \times 10^{-18} \text{s}^{-1}$	$ \ddot{P}_b = \frac{\ddot{\omega}^S P_b^2}{2\pi} \sim 5 \times 10^{-19} \text{s}^{-1}$
$ \ddot{\ddot{P}}_b ^{obs} < 3 \times 10^{-26} \text{s}^{-2}$	$ \ddot{\ddot{P}}_b = \frac{P_b^2}{2\pi} \frac{d^4 \omega^S}{dt^4} \sim 1 \times 10^{-26} \text{s}^{-2}$

In the estimation of parameters in this table, $c_1 = 1$, $c_2 = 10^2$ and $c_3 = 10^4$ is assumed.

TABLE V: Measured parameters compare with the geodetic precession induced ones in PSR J1012+5307

observation	this paper
$ \dot{x} ^{obs} < 1.4 \times 10^{-14}$	$\dot{x} = \dot{x}^{obs}$
$\dot{P}_b^{obs} = 1 \times 10^{-13}$	$ \dot{P}_b = \left \frac{\dot{\omega}^S P_b^2}{2\pi} \right \sim 4 \times 10^{-13}$

In the estimation of parameters in this table, $c_1 = 1$ is assumed.

TABLE VI: Measured parameters compare with the geodetic precession induced ones in PSR J1713+0747

observation	this paper
$ \dot{x} ^{obs} = 5(12) \times 10^{-15}$	$\dot{x} = \dot{x}^{obs}$
$\dot{P}_b^{obs} = 1(29) \times 10^{-11}$	$ \dot{P}_b = \left \frac{\dot{\omega}^S P_b^2}{2\pi} \right \sim 1 \times 10^{-10}$

In the estimation of parameters in this table, $c_1 = 1$ is assumed.

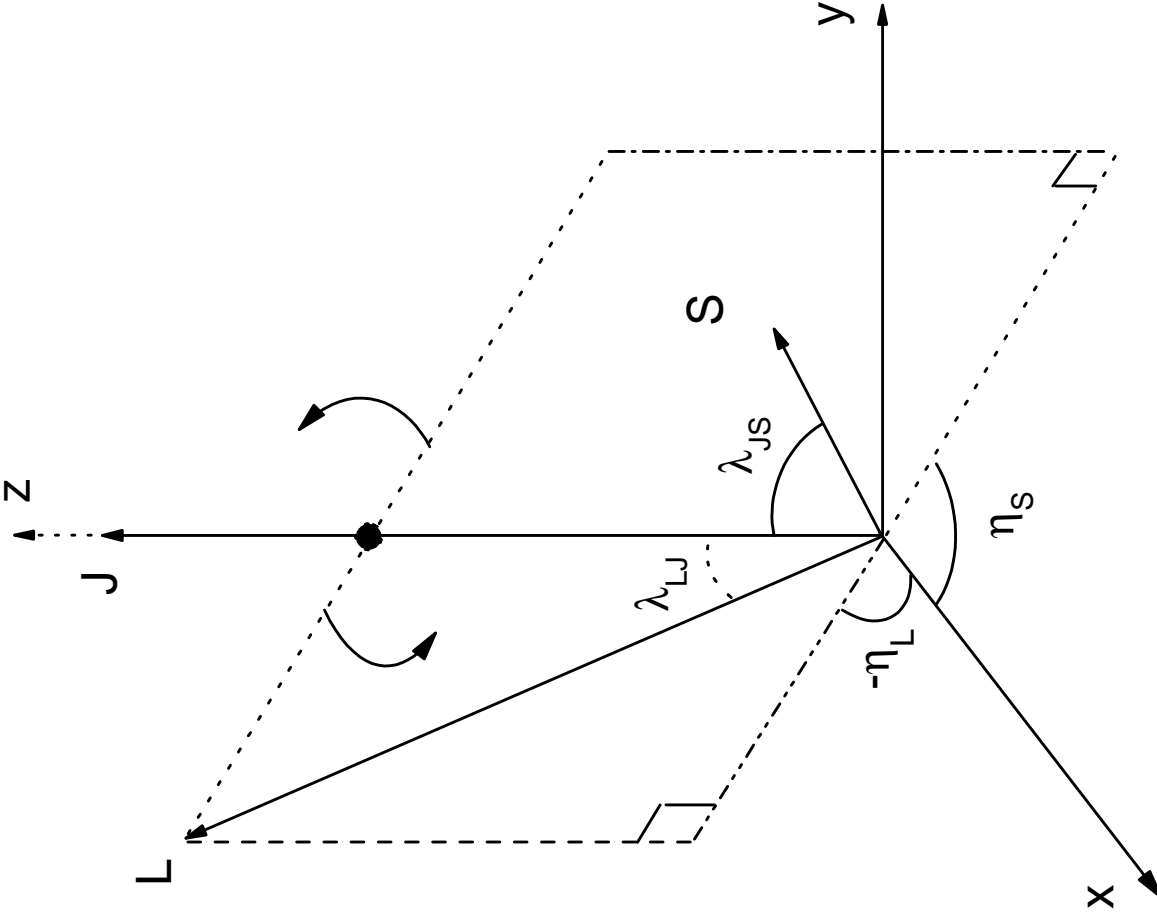


FIG. 1: In 1PN, the scenario of motion of a binary pulsar system can be described as the rotation of the plane determined by \mathbf{L} , \mathbf{S} around the fixed axes, \mathbf{J} . η_L and η_S are precession phases of \mathbf{L} and \mathbf{S} in the \mathbf{J} -coordinate system respectively.

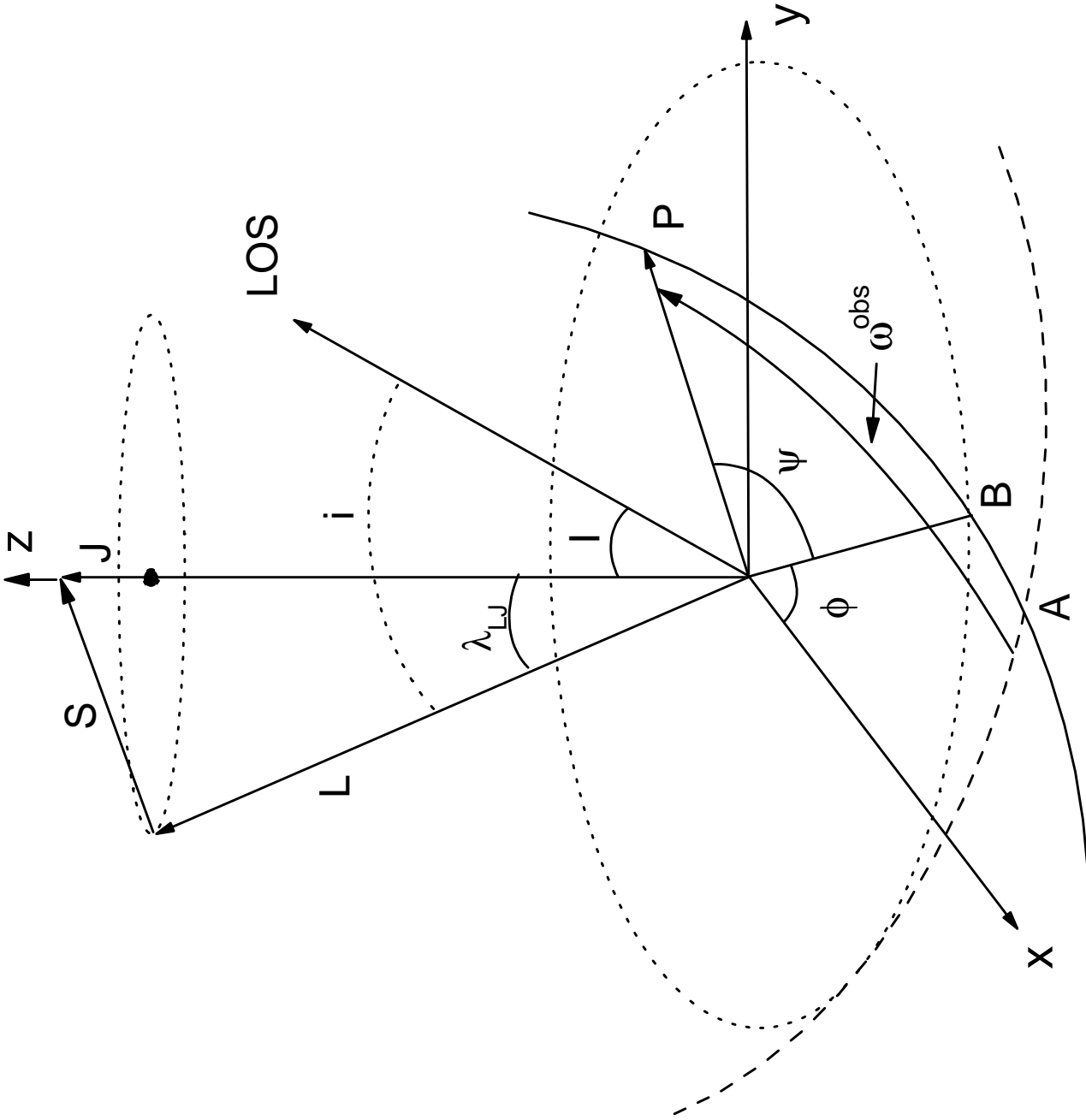


FIG. 2: Binary geometry and definitions of angles. The invariable plane (x - y), which is represented by the dotted ellipse, is perpendicular to the total angular momentum, \mathbf{J} . The inclination of the orbital plane with respect to the invariable plane is λ_{LJ} , which is also the precession cone angle of \mathbf{L} around \mathbf{J} . The orbital inclination with respect to the line of sight is i . ϕ (Ω) is the phase of the orbital plane precession. ψ (ω) is longitude of periastron from point B, and ω^{obs} is longitude of periastron from point A.

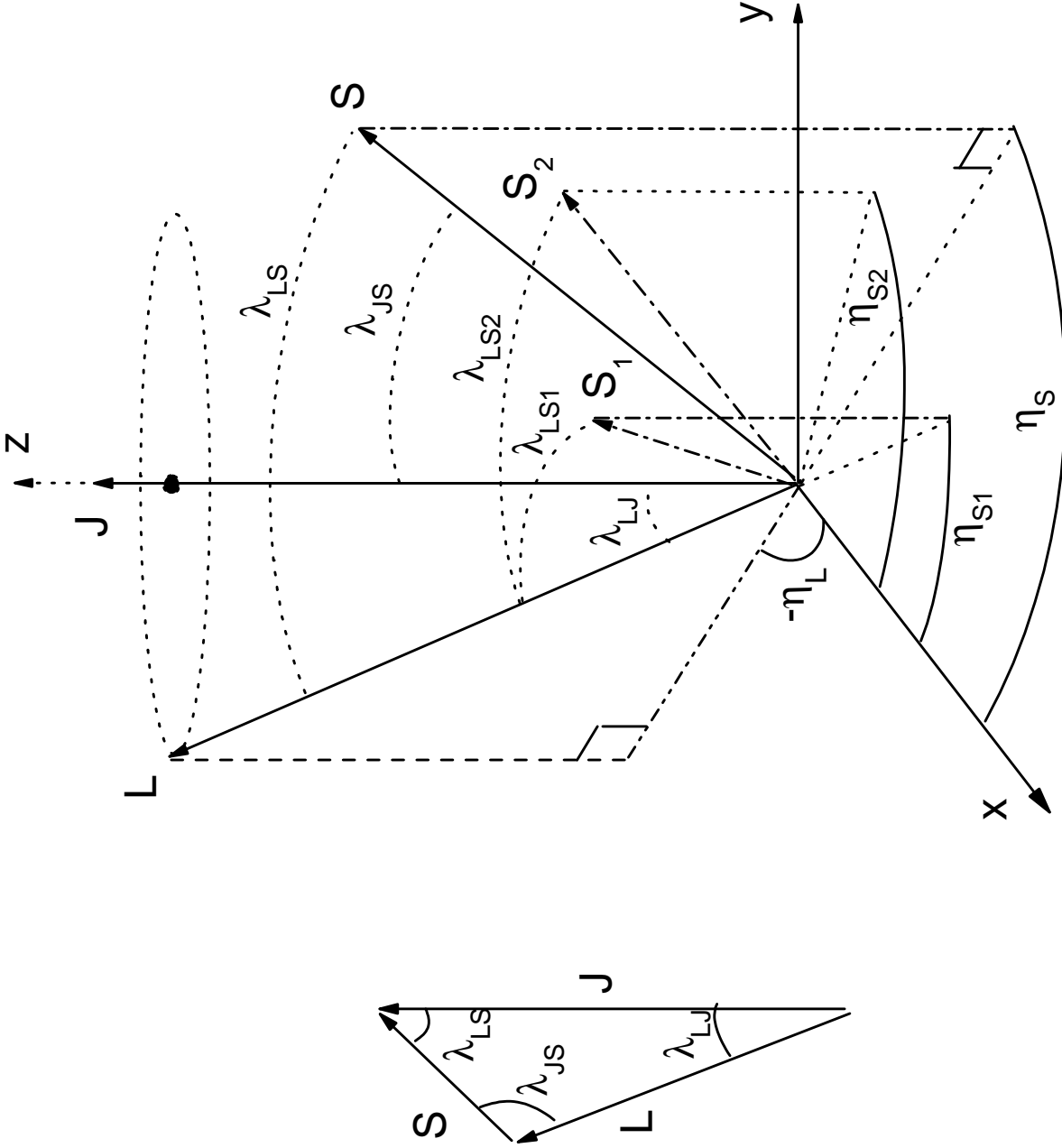


FIG. 3: Angles and orientation conventions relating vectors, \mathbf{S} , \mathbf{L} and \mathbf{J} to the coordinate system. x - y is the invariance plane, η_{S1} , η_{S2} , η_S and η_L are precession phases of \mathbf{S}_1 , \mathbf{S}_2 , \mathbf{S} and \mathbf{L} respectively.